ULTRASHORT LASER PULSE PROPAGATION IN WATER

A Thesis

by

JOONG-HYEOK BYEON

Submitted to the Office of Graduate Studies of
Texas A&M University
in partial fulfillment of the requirements for the degree of

MASTER OF SCIENCE

August 2008

Major Subject: Physics

ULTRASHORT LASER PULSE PROPAGATION IN WATER

A Thesis

by

JOONG-HYEOK BYEON

Submitted to the Office of Graduate Studies of
Texas A&M University
in partial fulfillment of the requirements for the degree of

MASTER OF SCIENCE

Approved by:

Chair of Committee,	George W. Kattawar
Committee Members,	Alexei Sokolov
	Ping Yang
Head of Department,	Edward Fry

August 2008

Major Subject: Physics

ABSTRACT

Ultrashort Laser Pulse Propagation in Water. (August 2008)

Joong-Hyeok Byeon, B.S., Ajou University;

M.S., Seoul National University

Chair of Advisory Committee: Dr. George W. Kattawar

We simulate ultrashort pulse propagation through water by numerical methods, which is a kind of optical communication research. Ultrashort pulses have been known to have non Beer-Lambert behavior, whereas continuous waves (CW) obey the Beer-Lambert law. People have expected that the ultrashort pulse loses less intensity for a given distance in water than CW which implies that the pulse can travel over longer distances. In order to understand this characteristic of the pulse, we model numerically its spectral and temporal evolution as a function of traveling distance through water. We achieve the pulse intensity attenuation with traveling distance, obtain the temporal envelope of the pulse and compare them with experimental data. This research proves that the spectral and temporal profile of a pulse can be predicted knowing only the intensity spectrum of the input pulse and the refractive index spectrum of water in the linear regime. The real feasibility and the advantage of using an ultrashort pulse as a communication carrier will also be discussed.

To My Family

ACKNOWLEDGEMENTS

I would like to express my appreciation for Dr. George W. Kattawar's guidance of my study as my academic advisor for one year and a half. He always gives sincere answers and educates me with great patience.

I also appreciate Dr. Alexei Sokolov. Even though he is leading experiments, he always gives me innovative ideas for my simulation research.

I would like to thank Dr. Ping Yang. He always shows interest in my research and advices me.

I thank all of my office mates; Dr. Pengwang Zhai, Dr. Yu You, and Mr. Lei Bi. Whenever I face some difficulties or problems in my work, they always help me and do not hesitate to share their knowledge and ideas.

I never forget my former academic advisor's, Dr. Peter M. McIntyre, favors. He allowed me to experience many research studies. Those are my big intellectual properties.

I thank my parents and parents-in-law. They always support us both materially and morally.

Finally, I'd like to express my heartfelt thanks to my beloved wife, Seong-Hey Seo and my dear daughter, Ye-Young Byeon. They are my life itself.

TABLE OF CONTENTS

LIST OF FIGURES

LIST OF TABLES

CHAPTER I

INTRODUCTION AND BACKGROUND

As femtosecond laser pulse technology has developed [1], studies of ultrashort pulse propagation through a linear dielectric medium such as water [2, 3, 4] are now just beginning to be explored. A continuous wave (CW) has been the main communication carrier until this time. However it attenuates exponentially in water because it follows the Beer-Lambert law. On the other hand, an ultrashort pulse has been reported to have non Beer-Lambert behavior [5]. The attenuation of the transmitted intensity of the pulse is less than a CW for a given distance. This characteristic of the pulse has attracted a great deal of attention in optical communication research even though it is known as a linear phenomenon. The objective of this thesis is to understand this characteristic of the pulse using numerical computation. We will model ultrashort pulse propagation through water and obtain the spectral and temporal evolution of the pulse along the water path length, taking into account the complete refractive index dispersion of water. First of all, we need to understand the following basic concepts.

A. Beer-Lambert Law

The Beer-Lambert law states the linear relationship between the absorbance and the product of the absorption coefficient and the path length of a medium.

The journal model is Optics Express.

There is a logarithmic dependence between absorbance and transmissivity of light, which is an empirical relationship.

$$A = \sigma N l = \alpha l$$
$$A = -\ln\left(\frac{I_t}{I_i}\right) \tag{1.1}$$

where A is an absorbance, I_t is the transmitted intensity, I_i is the initial intensity.

σ is an absorption cross section, (m^2)

N is the number density of absorbers. (N/m^3)

l is traveling distance . (1/m)

α is an absorption coefficient (1/m)

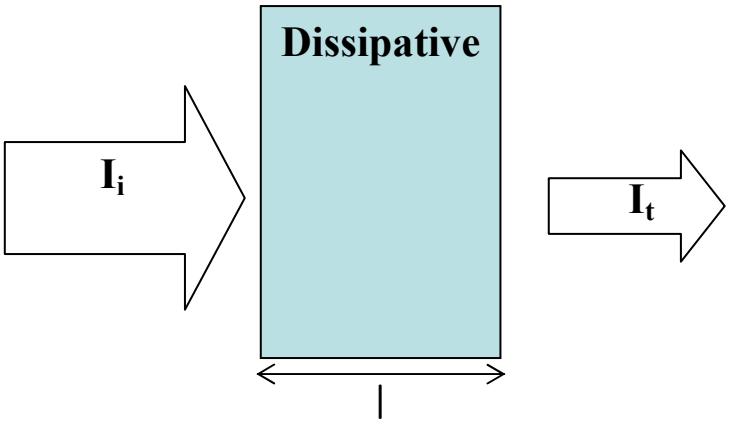

Fig. 1. Intensity attenuation through dissipative medium

The Beer-Lambert law describes the amount of the intensity that is lost by the light as it propagates through a dissipative medium. A continuous wave has a single frequency component and follows the Beer-Lambert law, whereas a pulse does not [5]. What physical difference causes this discrepancy? We will seek the answer through this research.

B. Ultrashort pulse as communication carrier

Even though the term "Ultrashort" is not defined commonly, if the pulse duration is on the order of femtoseconds or shorter, it is called an ultrashort pulse. Its duration time is much shorter than the reorientational relaxation time of water molecules [6], which is on the order of picoseconds.

The non Beer-Lambert characteristic of the ultrashort pulse gives new perspective to communication studies. An ultrashort pulse is supposed to survive longer and travel further than a continuous wave. Why does the pulse behave in such a way? Is it a kind of simple interaction between the pulse and water? Does the ultrashort pulse have an advantage over continuous waves? We will answer these questions by numerically modeling the spectral and temporal evolution of an ultrashort pulse in water with distance. The spectral evolution will give the transmitted intensity spectrum and we can obtain the intensity attenuation from that. The temporal profile reveals how the dielectric character of a medium affects the pulse. This study will find numerical methods to simulate ultrashort pulse propagation through water, obtain the spectral and temporal evolution of the pulse over traveling distance through water and compare the results with experimental data.

CHAPTER II

SIMULATION METHODS

A. Finite-difference time-domain method

The finite-difference time-domain (FDTD) method is one of the most powerful and popular numerical computational techniques for electrodynamics [8, 9, 10, 11]. As expected from its nomenclature, it provides the spatial and temporal solution of the electromagnetic field, which propagates in a dielectric medium and interacts with a dielectric system. It can also be applied to photonic and optoelectronic device simulation [12, 13]. With the advent of high speed computers, FDTD is used much more broadly. We will review the FDTD method briefly and seek the way in which we can apply it to our research.

1. FDTD formula in a non-dissipative medium

The strongest point of the FDTD technique is that it seeks a temporal and spatial solution by directly solving Maxwell equations in the time domain. The time dependent Maxwell equations in a dielectric medium without a current source are given by:

$$\nabla \times \mathbf{H} = \varepsilon\varepsilon_0 \frac{\partial \mathbf{E}}{\partial t}$$
$$\nabla \times \mathbf{E} = -\mu_0 \frac{\partial \mathbf{H}}{\partial t} \qquad (2.1)$$

where ε_0 and μ_0 are the vacuum electric permittivity and magnetic permeability respectively, and ε is the relative permittivity, a pure real value and independent of time.

Actually the magnitude difference between **E** and **H** is several orders since ε_0 and μ_0 differ by that magnitude, which is inconvenient for numerical computation. We adopt the following change of variables in order to remove this inconvenience [9].

$$\bar{\mathbf{E}} = \sqrt{\frac{\varepsilon_0}{\mu_0}}\mathbf{E} \tag{2.2}$$

Substituting Eq. 2.2 into Eq. 2.1 gives

$$\begin{aligned} \nabla \times \mathbf{H} &= \frac{\varepsilon}{c}\frac{\partial \bar{\mathbf{E}}}{\partial t} \\ \nabla \times \bar{\mathbf{E}} &= -\frac{1}{c}\frac{\partial \mathbf{H}}{\partial t} \end{aligned} \tag{2.3}$$

For simplicity, a one-dimensional case using only $\mathbf{E}_x$ and $\mathbf{H}_y$ will be considered. Eq. 2.3 reads

$$\begin{aligned} \frac{\partial H_y}{\partial z} &= -\frac{\varepsilon}{c}\frac{\partial \bar{E}_x}{\partial t} \\ \frac{\partial \bar{E}_x}{\partial z} &= -\frac{1}{c}\frac{\partial H_y}{\partial t} \end{aligned} \tag{2.4}$$

They are the plane wave equations of the electric field and the magnetic field propagating in the z direction, pointing the x and y directions respectively. Discretizing them by the central difference approximation for both the temporal and spatial derivatives gives [11]

$$\begin{aligned} -\frac{H_y^n(k+1/2) - H_y^n(k-1/2)}{\Delta z} &= \frac{\varepsilon}{c}\frac{\bar{E}_x^{n+1/2}(k) - \bar{E}_x^{n-1/2}(k)}{\Delta t} \\ \frac{\bar{E}_y^{n+1/2}(k+1) - \bar{E}_y^{n+1/2}(k)}{\Delta z} &= \frac{1}{c}\frac{H_y^{n+1}(k+1/2) - H_y^n(k+1/2)}{\Delta t} \end{aligned} \tag{2.5}$$

where n, the temporal index means a time $t = \Delta t \cdot n$

k, the spatial index means the distance $z = \Delta z \cdot k$.

As Eq. 2.5 indicates, **E** and **H** are not calculated at the same time nor at the spatial position. One field (**E**) values are located between the other field (**H**) values. This interweaving arrangement makes each derivative of the fields match at the same temporal and spatial position.

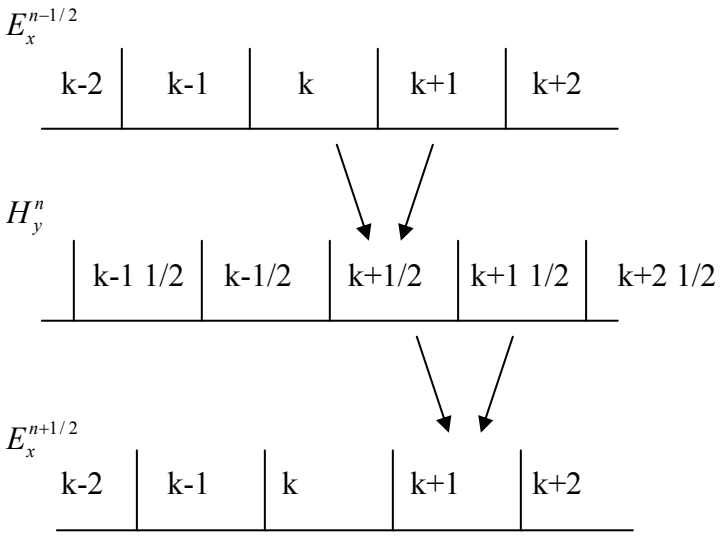

Fig. 2. Interweaving of both fields in space and time in the FDTD equation [11].

Discretized expressions for an iterative algorithm are

$$\begin{aligned} \bar{E}_x^{n+1/2}(k) &= \bar{E}_x^{n-1/2}(k) - \frac{1}{\varepsilon}\frac{1}{S}\left[H_y^n(k+1/2) - H_y^n(k-1/2)\right] \\ H_y^{n+1}(k+1/2) &= H_y^n(k+1/2) - \frac{1}{\varepsilon}\frac{1}{S}\left[\bar{E}_y^{n+1/2}(k+1) - \bar{E}_y^{n+1/2}(k)\right] \end{aligned} \tag{2.6}$$

where $S = \dfrac{c\Delta t}{\Delta z}$

The above FDTD formulation shows that the new **E** field value ($E_x^{n+1/2}$) at the position k is calculated from the previous **E** field value ($E_x^{n-1/2}$) at the position k and the most recent **H** values at the position k+1/2 and the position k-1/2. Such repeating iterative process will give the temporal and spatial evolution of the field at any desired time and position. It is the basic algorithm of the grid-based differential time-domain numerical modeling technique [8].

$S = \frac{c\Delta t}{\Delta z}$ is the numerical stability factor [10] (or Courant number). A spatial grid (space increment) and a time-step should be chosen so that the simulation ensures numerical stability. They must satisfy the following Courant-Friedrichs-Levy (CFL) condition.

$$S = \frac{c\Delta t}{\Delta z} \le 1 \tag{2.7}$$

For example, If S=1/2, Eq. 2.7 reads $2\Delta t = \frac{\Delta z}{c}$ meaning that it takes two time steps for a wave to propagate one space step. If S=1/3, it takes three time steps. One can easily understand without mathematical proof that the more time steps that are taken to reach some distance, the more stable a numerical computation can be achieved. This is the reason why S is called the numerical stability factor. However, the total computation time is inversely proportional to S. The higher accuracy can be achieved by reducing grid size, Δz , however it also increases the total computation time.

2. FDTD formula in a dissipative medium

A dissipative or absorptive medium gives ε a non zero imaginary part. So $\varepsilon = \varepsilon_r + i\varepsilon_i$. Eq. 2.6 reads [14] with a little algebra.

$$\begin{aligned} \bar{E}_x^{n+1/2}(k) &= \exp[-\bar{\tau}\Delta t]\bar{E}_x^{n-1/2}(k) - \frac{1-\exp[-\bar{\tau}\Delta t]}{\bar{\tau}\Delta t\varepsilon_i}\frac{1}{S}\left[H_y^n(k+1/2) - H_y^n(k-1/2)\right] \\ H_y^{n+1}(k+1/2) &= \exp[-\bar{\tau}\Delta t]H_y^n(k+1/2) - \frac{1-\exp[-\bar{\tau}\Delta t]}{\bar{\tau}\Delta t\varepsilon_i}\frac{1}{S}\left[\bar{E}_y^{n+1/2}(k+1) - \bar{E}_y^{n+1/2}(k)\right] \end{aligned} \tag{2.8}$$

where $\bar{\tau} = \dfrac{kc\bar{\varepsilon}_i}{\bar{\varepsilon}_r}$, $\quad k = \dfrac{2\pi}{\lambda}$, $\quad \bar{\varepsilon}_i$ & $\bar{\varepsilon}_r$: averages of ε_i & ε_r of two adjacent grids.

B. Fourier Superposition method

Since this research is conducted in a linear regime, the linear superposition principle can be used for numerical computation. As long as a pulse propagates only in one dimension without scatterings, the detailed information of its initial spectrum can be given, the Fourier Superposition (FS) method is a good choice for fast calculation. In order to obtain the temporal evolution of propagating pulses, we need to superpose fields in the frequency domain.

$$\begin{aligned} \mathbf{E}_x(z,t) &= \frac{1}{\sqrt{2\pi}}\int_{-\infty}^{\infty}\mathbf{E}_\omega(z,\omega)\exp[-i\omega t]d\omega \\ &= \frac{1}{\sqrt{2\pi}}\int_{-\infty}^{\infty}\mathbf{E}_\omega(z=0,\omega)\exp[ikz - i\omega t]d\omega \end{aligned} \tag{2.9}$$

$$k(\omega) = \frac{\omega}{c}\left(n_r(\omega) + in_i(\omega)\right) = n_r(\omega)\frac{\omega}{c} + i\frac{\alpha(\omega)}{2} \tag{2.10}$$

where $n_r(\omega)$: the real part of refractive index,

$n_i(\omega)$: the imaginary part , $\alpha(\omega)$: the absorption coefficient.

Once the spectrum of the refractive index is given and scatterings can be neglected, the intensity spectrum, the total intensity and the temporal evolution of propagating pulses can be numerically calculated. The Beer-Lamber law can also be derived from the above equation.

$$\mathbf{E}_{\omega}(z,\omega) = \mathbf{E}_{\omega}(0,\omega)\exp[ikz] \tag{2.11}$$

$$I_{\omega}(z,\omega) = \mathbf{E}_{\omega}(z,\omega)\mathbf{E}^{*}_{\omega}(z,\omega) \text{ : Intensity} \tag{2.12}$$

$$= \mathbf{E}_{\omega}(0,\omega)\mathbf{E}^{*}_{\omega}(0,\omega)\exp[-\alpha(\omega)z]$$

$$= I_{0\omega}(\omega)\exp[-\alpha(\omega)z]$$

$$I_{\omega}(z,\omega) -> I_{\lambda}(z,\lambda)$$

$$I_{\lambda}(z,\lambda) = I_{\lambda}(0,\lambda)\exp[-\alpha(\lambda)z] \quad \text{: the Beer-Lambert law} \tag{2.13}$$

$$I_{t}(z) = \int_{0}^{\infty} I_{\lambda}(0,\lambda)\exp[-\alpha(\lambda)z]d\lambda$$

where $\alpha(\lambda)$ is the wave length dependent absorption coefficient.

$I_{\lambda}(0,\lambda)$ is the initial intensity spectrum and $I_t(z)$ is the total intensity at path distance z.

Österberg [5] measured the intensity spectra of the transmitted ultrashort laser pulse through water at different path lengths and predicted theoretically those spectra and the total intensity attenuations by Eq. 2.13.

Several other groups [2, 15] also measured and calculated the total transmitted intensity attenuations by Eq. 2.13. There is good correlation between the measured data and the calculations.

C. Refractive index of water

Both of the above methods require the wavelength (or frequency) dependent refractive index for numerical computation. The imaginary part is directly related to the absorption coefficient. The measured imaginary part of Pope [16] and Kou [17] will be used. The real part is calculated from the refractive index spectrum formulation [18] adopted by the International Association for the Properties of Water and Steam (IAPWS) [19].

$$\frac{n_r^2-1}{n_r^2+2} = a_0 + a_1\overline{\rho} + a_2\overline{T} + a_3\overline{\lambda}^2\overline{T} + \frac{a_4}{\overline{\lambda}^2} + \frac{a_5}{\overline{\lambda}^2-\overline{\lambda}_{UV}^2} + \frac{a_6}{\overline{\lambda}^2-\overline{\lambda}_{IR}^2} + a_7\overline{\rho}^2 \qquad (2.14)$$

where dimensionless variable and reference constants

Density : $\overline{\rho} = \rho/\rho^*$, $\rho^* = 1000$ kg m^{-3}

Temperature : $\overline{\mathrm{T}} = T/T^*$, $T^* = 273.15K$ and Table 1.

Wavelength : $\overline{\lambda} = \lambda/\lambda^*$, $\lambda^* = 0.589\ \mu$m

Table 1. Coefficients of Eq. 2.14

$a_0 = 0.244\ 257\ 733$	$a_4 = 1.580\ 205\ 70\times10^{-3}$
$a_1 = 9.746\,344\,76\times10^{-3}$	$a_5 = 2.459\ 342\ 59\times10^{-3}$
$a_2 = -3.732\ 349\ 96\times10^{-3}$	$a_6 = 0.900\ 704\ 920$
$a_3 = 2.686\ 784\ 72\times10^{-4}$	$a_7 = -1.666\ 262\ 19\times10^{-2}$
$\overline{\lambda}_{UV} = 0.299\ 202\ 0$	$\overline{\lambda}_{IR} = 5.432\ 937$

The FDTD method uses relative permittivity. The real part and the imaginary part of relative permittivity can be calculated by the following formulas.

$n_i = \frac{\alpha\lambda}{4\pi}$ where α is the absorption coefficient.

$\varepsilon = \varepsilon_r + i\varepsilon_i$

$\varepsilon_r = n_r^2 - n_i^2$

$\varepsilon_i = 2n_r n_i$

Figure. 3 displays the measured absorption coefficient and the calculated refractive index.

As seen Fig. 3, the variation of the real part of the refractive index in this spectral range is less than 2%, however, its effect on the temporal profile is large.

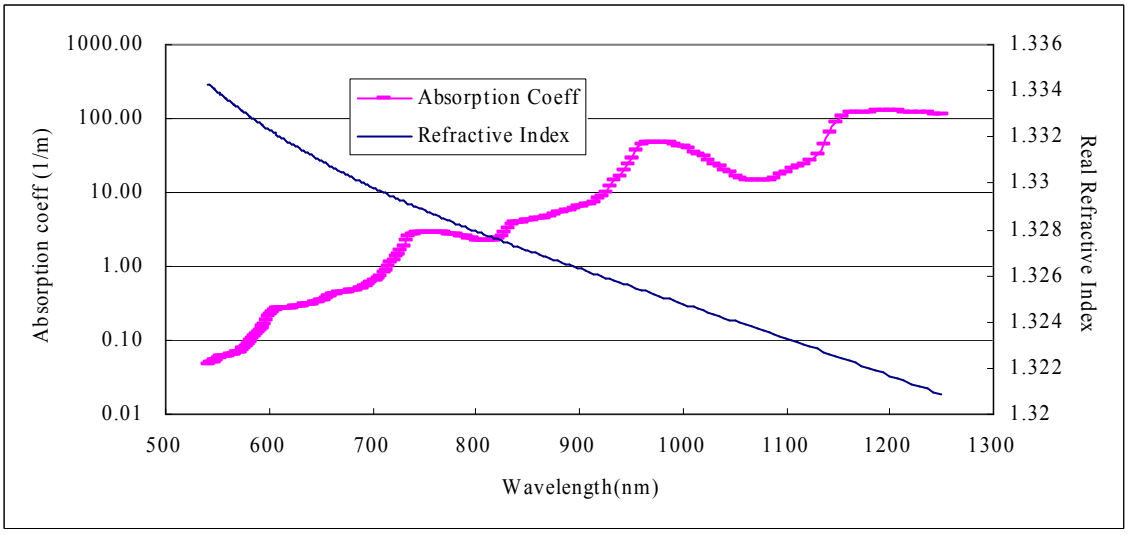

Fig. 3. The absorption coefficient [17] and the real refractive index [18] spectrum.

The absorption coefficient and the imaginary part of the refractive index tell us how an electromagnetic wave loses its energy as it propagates through a dissipative medium. So the total intensity decreases and the profile of the intensity spectrum shrinks as a wave travels through the dissipative medium. They also affect the temporal profile of the wave. The real refractive index is defined as the ratio of the vacuum phase velocity to the phase velocity in the medium. The wavelength dependence of the real refractive index means that each wave component has a different phase velocity. Since the real part does not lead to energy loss, the intensity spectrum profile is unchanged; however, the temporal profile of the pulse varies as it propagates in water. It is common for the temporal and spatial width of the pulse envelope to spread as it travels in a dispersive medium.

D. Simulation example

A simple example is given and will be simulated by the FDTD and the FS methods. A 10fs Gaussian wave pulse centered at 755nm will propagate in water. Because the FDTD method solves the equations in time and space, the simulation process is the same as reality. This pulse is generated in a vacuum, travels in one dimension, is incident on water and propagates through water. (see Figure 4 (a)) FDTD needs an initial pulse spectrum and the spectrum of the relative permittivity. The simulation parameters are

$$S = \frac{c\Delta t}{\Delta z} = 1, \quad \Delta z = \frac{\lambda_c}{20}, \ \lambda_c = 750nm$$

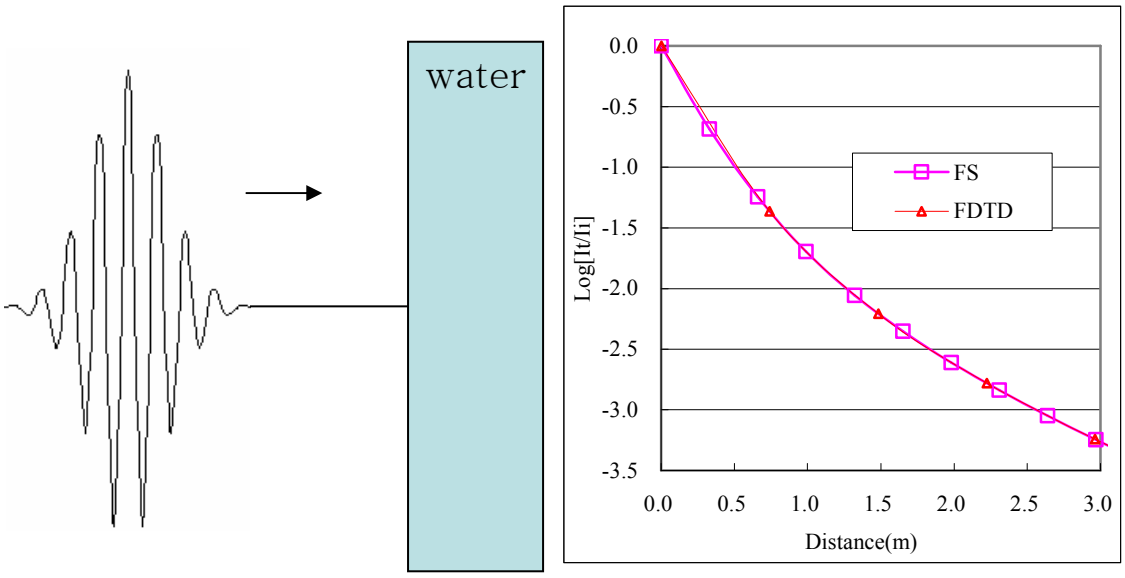

(a) Simulation example (b) Results of FDTD & FS

Fig. 4. An example of simulation and results.

The intensities were calculated by $|\mathbf{E}_x|^2$ at given distances.

We simulate the same propagation by the FS method which needs the spectrum of the absorption coefficient. As seen in Figure 4 (b), both results coincide with each other. The ultrashort pulse reveals the non Beer-Lambert behavior as expected [5].

CHAPTER III

RESULTS AND CONCLUSION

A. Intensity attenuation of a pulse

1. Experimental data and simulation results

Our experimental group measured the transmitted pulse intensity spectra for a series of propagation distances (0.5~2.5m). They provided the total transmitted intensity attenuation of the passing distance through water. A laser pulse of 30fs, 80Mhz, was employed (see Figure 5 (a)). The E-field amplitude spectrum was calculated from the input intensity spectrum for the initial condition of the FDTD method (see Figure 5 (b)).

Since a pulse in the time domain is the sum of an infinite number of discrete single frequency components, we calculated 200 discrete single frequency solutions in the pulse spectrum range and then added them together to find the temporal solution. We included only the imaginary part of the relative permittivity because we had the measured absorption data of the pulse.

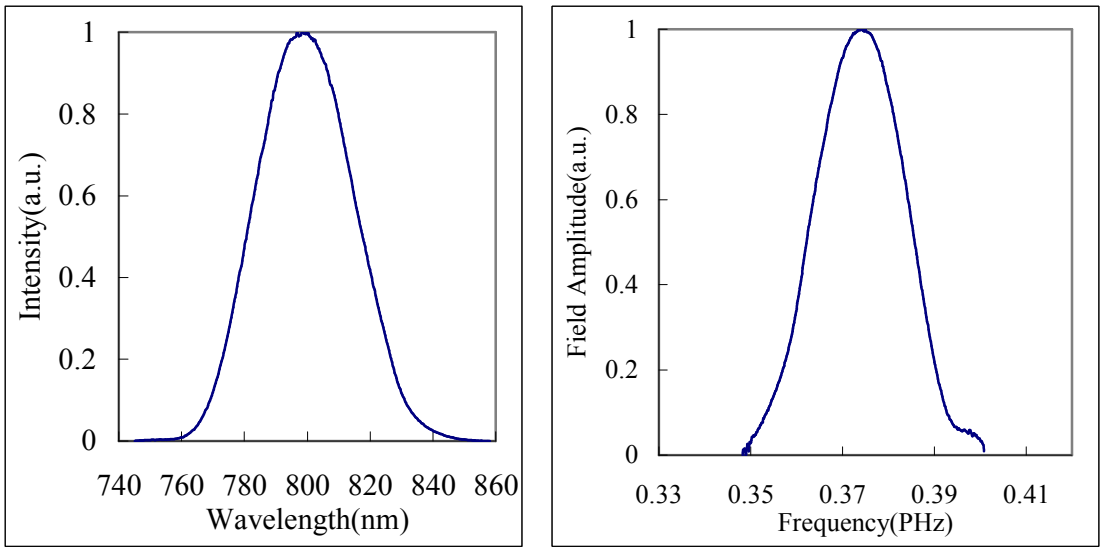

(a) (b)

Fig. 5. The spectrums of the initial intensity and field measured by Lucas Naveira and Dr. Alexie Sokolov.

(a) The intensity spectrum of the input pulse.

(b) Calculated E-field amplitude spectrum from (a). $|\mathbf{E}| = \sqrt{I}$

Pulse in time domain $= \mathbf{E}_t(x,t) = \sum_i \mathbf{E}_f(x, f_i) e^{-i2\pi f_i t}$

We calculated the total intensities at given passing distances by $I(x) = \sum_t |\mathbf{E}(x,t)|^2$ (see Figure 6)

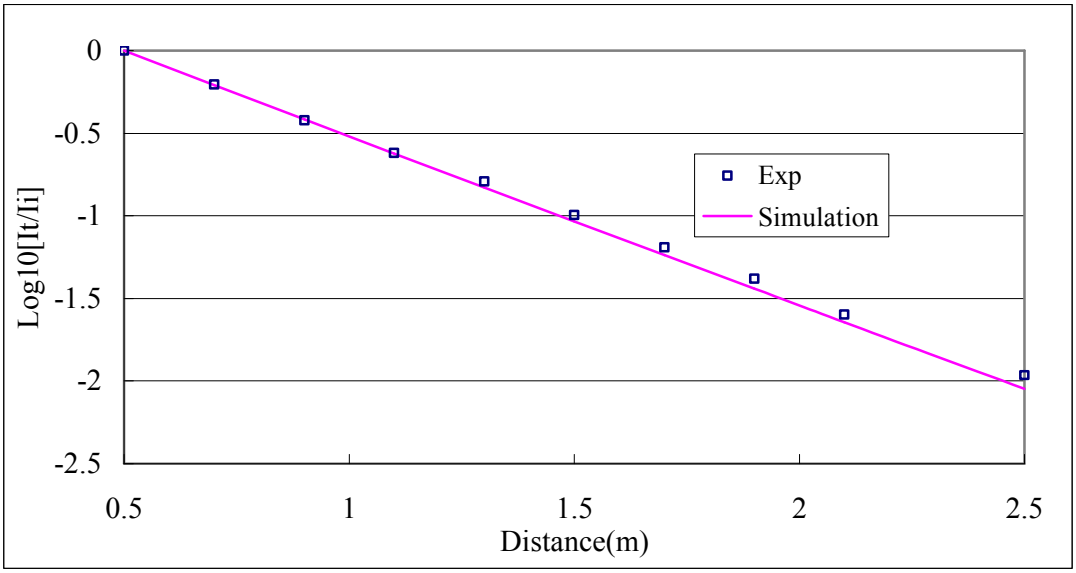

Fig. 6. Attenuations of measured and predicted intensities.

The X-axis is the path length through water.

The Y axis is the ratio of the transmitted intensity to the input intensity on a Log10 scale.

As Figure 6 displays, even though the predicted absorption of the pulse is more than the measured absorption, it shows a similar trend. Like a continuous wave, the attenuation line of the pulse is straight on a Log10 scale. We defined an effective absorption coefficient of the pulse and calculated it from the above results by the least squares fitting as shown in Table 2. We found an error of 4.2%. This low error validates our experimental group's good experimental technique.

Table 2. Extracted effective absorption coefficients

Our group's experimental data	2.2578 (1/m)
Simulation result	2.3584 (1/m)

The absorption coefficients were extracted from our experimental data as the next step and compared to Kou's data [17].

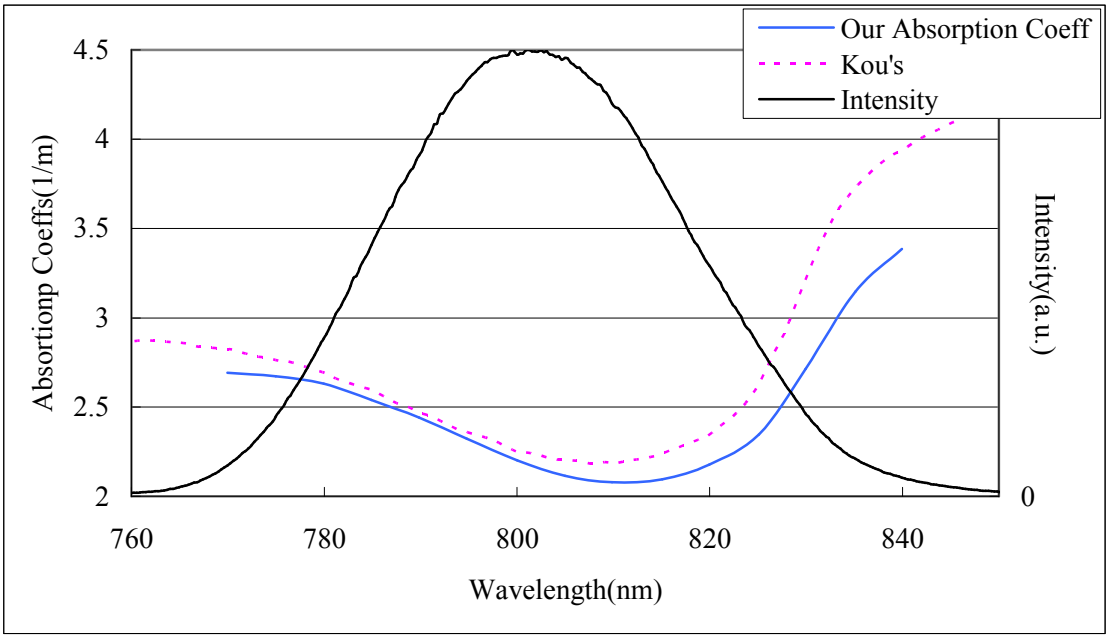

Fig. 7. Extracted absorption coefficients from the measured spectra of intensity attenuations.

Kou used CW instead of pulses, measured the transmission and derived the Beer-Lambert absorption coefficients. He calculated them precisely by eliminating all possible

experimental errors, whereas we simply used the Beer-Lambert formula without refining the measured data. As seen in Figure 7, our absorption coefficients are lower than Kou's data up to 5% in the main power spectral range, 780~ 830nm. The difference may be due to water quality and the experimental scheme. For this reason, the measured intensity attenuation is less than the predicted attenuation.

2. Conclusion

The measured absorption function for our pulse with the water path distance is different from what we expected. The intensity of our 30fs pulse attenuates exponentially, which is the same as continuous waves. However, the attenuation of the 10fs pulse is subexponential [5] as predicted in Fig. 4(b). The physical reason of that difference can be deduced by comparing the intensity spectra of the two pulses.

As Figure 8(a) indicates, the 10fs pulse has a broader spectral range than the 30fs pulse because the bandwidth is inversely proportional to the duration time of a pulse. Figure 8(b) shows that the curved attenuation line of the 10fs pulse is located between the straight attenuation lines of CW, 750nm and 650nm, which are in the spectral range of the 10fs pulse.

The subexponential attenuation of the 10fs pulse is due to the characteristics of an optical pulse. The pulse is the linear sum of an infinite number of continuous waves that obey the Beer-Lambert law. The 10fs pulse has more continuous components which have less absorption coefficients of the range of 600nm to 700nm than the 30fs pulse.

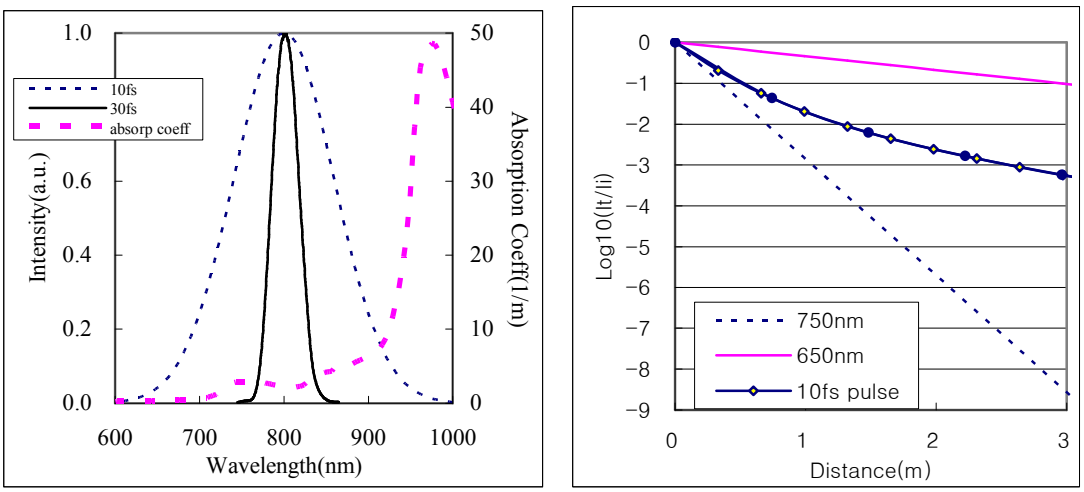

(a) (b)

Fig. 8. Input spectra of pulses and attenuation lines.

(a) Input Spectra of 10fs and 30fs pulses.

(b) Attenuation lines of pulses and continuous waves.

These lower attenuation components compensate for the intensity loss of higher absorptive components of the spectral range beyond 750nm. The compensation is the characteristic of the linear phenomenon and induces the subexponential attenuation of the 10fs pulse. On the other hand, the 30fs pulse has almost constant absorption coefficient values in its spectral range of 750nm~850nm. There is less compensation among continuous wave components composing the 30fs pulse. This is the reason why the intensity of the 30fs pulse attenuates exponentially.

People have believed that it is of great advantage to use ultrashort pulses as a communication carrier rather than continuous waves. Even though the pulse releases the subexponential attenuation of its intensity, some continuous wave components (600nm)

attenuate less than the ultrashort pulse (10fs pulse) as seen Figure 8(b). All short pulses do not have such forte. It depends on absorption coefficient values in its spectral range.

The optical precursor is an ideal candidate for a communication carrier, which has lower attenuation characteristic, however, no one has observed it yet.

B. Temporal profile of a pulse

1. Experimental data and simulation results

In order to investigate the temporal profile of a propagating pulse by numerical simulation, we had to include not only the imaginary part of the refractive index but also the real part. We used the Fourier Superposition method for fast computation. At first, the dispersion relation of water should be found, namely $k=k(\omega)$ and $\omega=\omega(k)$. The functional relationship between the wave vector and the angular frequency can be illustrated by the curve fitting in the graph.

Figure 9 indicates that k has a linear relationship with ω. The polynomial expression of one parameter in terms of the other parameter was derived.

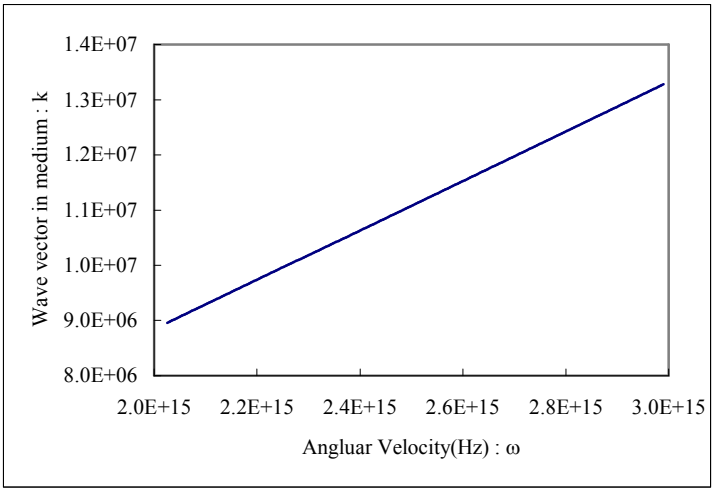

Fig. 9. The graph of the wave vector in water vs the angular velocity in the spectral range of our pulse.

$$\omega(k) = a_{k2} \cdot k^2 + a_{k1} \cdot k + a_{k0}$$
$$k(\omega) = a_{\omega 2} \cdot \omega^2 + a_{\omega 1} \cdot \omega + a_{\omega 0} \qquad (3.1)$$

where a_{k2}=-0.15981 (m^2/sec), $a_{k1}=2.26755\times10^{8}$ (m/sec), $a_{k0}=7.09636\times10^{12}$ (1/sec)

$a_{\omega 2}=1.84851\times10^{-26}$ (sec^2/m), $a_{\omega 1}=4.38991\times10^{-9}$ (sec/m), $a_{\omega 0}$=-10433.973 (1/m)

It should be noticed that there are nonzero $\frac{\partial^2\omega(k)}{\partial k^2}$ and $\frac{\partial^2 k(\omega)}{\partial\omega^2}$ terms, a_{k2} and $a_{\omega 2}$. They are directly related to Group Velocity Dispersion (GVD) parameter, D, which causes a pulse spread in time and space while it propagates in a dispersive medium.

$$D = -\frac{\lambda}{c}\frac{d^2 n_r}{d\lambda^2} = -\frac{2\pi c}{\lambda^2}\frac{d^2 k}{d\omega^2} = \frac{2\pi n^3}{\lambda^2 c^2}\left(1+\frac{\lambda}{n}\frac{dn}{d\lambda}\right)^3\frac{d^2\omega}{dk^2}$$

We can roughly estimate how wide the pulse envelope width spreads from Eq. 3.2 [20].

$$\Delta x(t) \simeq \sqrt{(\Delta x_0)^2 + \left(\frac{\omega'' t}{\Delta x_0}\right)^2} \tag{3.2}$$

where Δx_0 is a initial spatial width of the pulse.

When a 10fsec pulse passes through 1m of water, the calculated width is 124 times as wide as the initial width.

Österberg [3] measured the temporal evolution of a pulse which was thought to have a precursor behavior. Their initial 0.54 ps pulse was centered around 780nm with a bandwidth of 60nm. The pulse broke up and its temporal width spread up to 3ps after it propagated through 0.7m of deionized water. We simulated this pulse propagation with Österberg's given condition and the dispersion relation, Eq. 3.1.

As shown in Figure 10, our simulated pulse also reveals breakup after it propagated through 0.7m of water, however, its temporal width of 16ps is much wider than Österberg's 3ps.

Gaeta also simulated Österberg's pulse[15] (See Figure 11(a)). Österberg's pulse propagated over 0.7m at most, whereas Gaeta's result shows the pulse profile after 2.5m propagation. We repeated it with the same condition as Figure 10 (See Figure 11(b)).

There is still a significant difference in temporal widths. The width of our predicted pulse is twice as wide as Gaeta's width. Gaeta's refractive index formula is different from our formula. However, we used Gaeta's refractive index formula and obtained the same result as Figure 11(b).

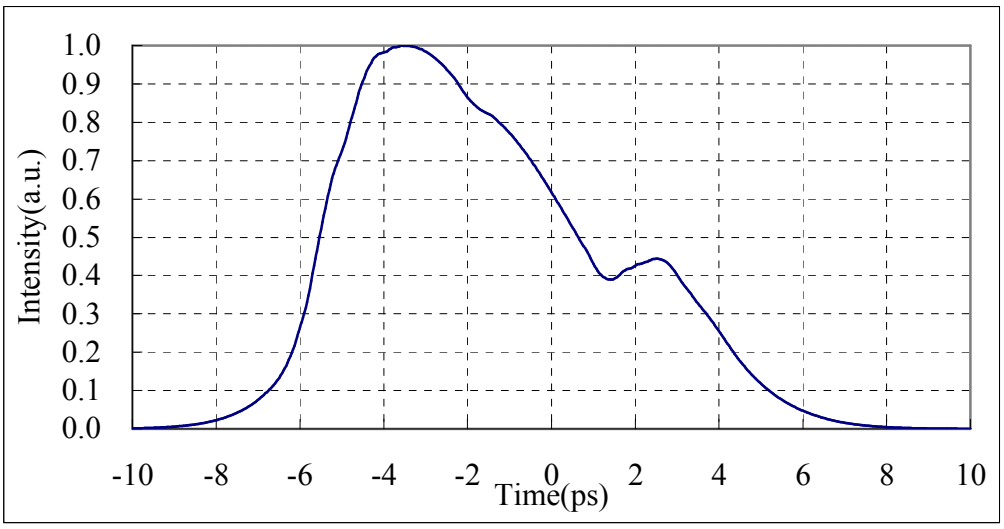

Fig. 10. The simulation result of Österberg's pulse. Even though the result shows the pulse breakup after 0.7m propagation, the temporal width is much wider.

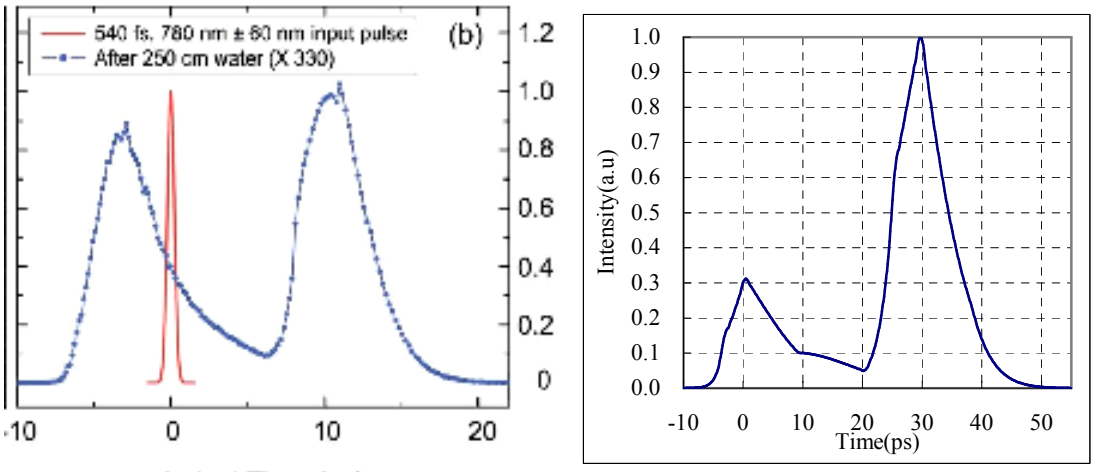

(a) Gaeta's simulation (b) Our simulation.

Fig. 11. Gaeta's simulation result. Gaeta modeled Österberg's pulse by Gaussian function in time domain adding a linear chip condition. (a) shows the temporal profile of the pulse after 2.5m propagation.

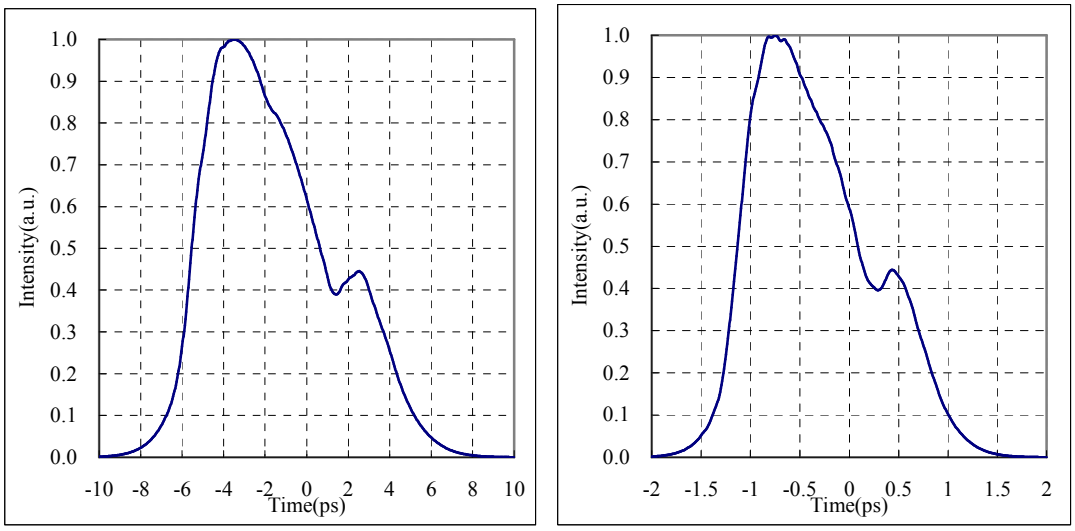

(a) $a_{\omega 2}=1.84851\times 10^{-26}$ (b) $a'_{\omega 2}=\frac{a_{\omega 2}}{5}$

Fig. 12. The simulation results with reduced GVD.

(a) Simulation with $a_{\omega 2}$ extracted from the IAPWS refractive index formula. Same as Figure 9.

(b) Simulation with a new reduced coefficient $a'_{\omega 2}=\frac{a_{\omega 2}}{5}$

To see the effect of the Group Velocity Dispersion on pulse propagation, we simulated it with a reduced coefficient, $a'_{\omega 2}=\frac{a_{\omega 2}}{5}$ (see Figure 12 (b)). The newly simulated pulse profile is compatible with the measured profile. The pulse breakup is mainly induced by the absorption process because both pulse shapes, Figure 12. (a) and (b) are the same even though the time scale changes. The temporal shape of the pulse itself can be predicted except for the time scale. The reduced coefficient $a'_{\omega 2}$ does not significantly affect the refractive index spectrum (see Figure 13). It makes the maximum

difference between two real refractive indexes 0.9%. This difference looks minor but its effect is large.

We found another temporal profile of the pulse from Alfano's paper [4]. His pulse had a 100nm spectral range and was centered at 790nm. We also simulated Alfano's experiment (Figure 14). We obtained better agreement with Alfano's results than Österberg's results. Figure 14 indicates that there is no pulse breakup like Österberg's.

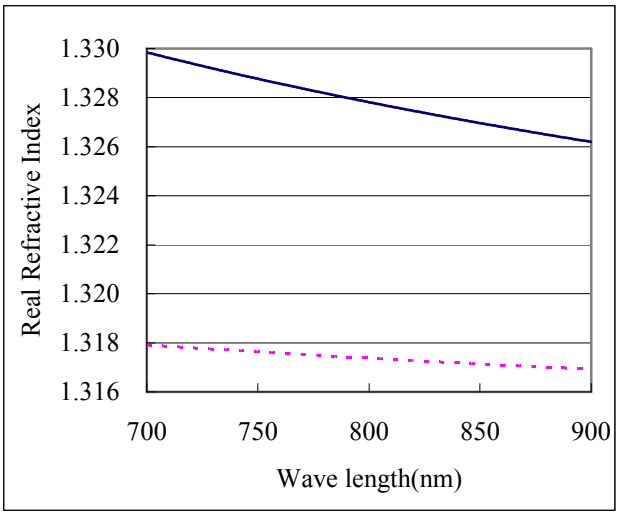

Fig. 13. Calculated refractive index with $a_{\omega 2}$ and $a'_{\omega 2} = \frac{a_{\omega 2}}{5}$.

The solid line and the dotted line represents $a_{\omega 2}$ and $a'_{\omega 2} = \frac{a_{\omega 2}}{5}$.

As Alfano mentioned, the spectrum profile and range critically determined the temporal shape. Even though we used the same refractive index spectrum as Österberg's case, the trends of simulations between two experimental data sets are different. We

need more temporal profile data of a pulse measured by experiment for further investigation.

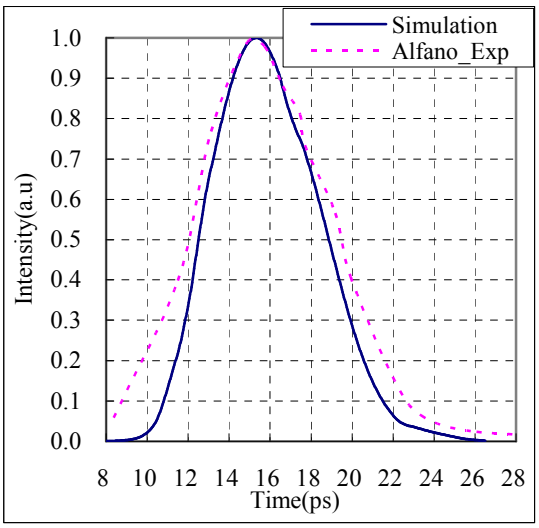

Fig. 14. The simulated results of Alfano's pulse. The solid line and the dotted line represent a simulated pulse and a measured one after 1.2m propagation.

2. Conclusion

We obtained temporal profiles of pulses and compared them with Österberg's and Alfano's experimental data which required the whole complex refractive index as the simulation parameters. It is clearly understood that the dispersion of real refractive index plays a role in changing the pulse profile. Even though there are some discrepancies between temporal widths of measured and the simulated pulse profiles, we can predict the shapes of propagating pulses except the temporal scales.

CHAPTER IV

SUMMARY

In this thesis, the physical characteristics of ultrashort pulse propagation in water were studied by numerical computation. An ultrashort pulse was found to attenuate subexponentially as it propagates in water in opposition to a continuous wave. In order to understand such behavior, we simulated ultrashort pulse propagation through water by the FDTD and the FS methods and obtained the total intensity attenuation and the temporal profile of the pulse as a function of the propagation distance.

The simulation results of the intensity attenuation agree with our experimental data. The precisely measured absorption coefficient data enabled us to model the pulse absorption process as well. The non-exponential decay of the pulse is induced by a compensation of the intensity loss among the CW components composing the pulse. Because the pulse is the sum of an infinite number of continuous waves which obey the Beer-Lambert law, the less absorptive components compensate for the intensity loss of high absorptive components. However, the subexponential attenuation of the ultrashort pulse does not always mean less decay than continuous waves.

We investigated how the real part and the imaginary part of the refractive index affect the pulse profile by modeling the temporal profiles of the pulses. The temporal width of the pulse increases as it travels through water due to the dispersive effects induced by the non constant real part. The absorption process determines the shape of the temporal pulse profile. In spite of discrepancies between temporal widths of the measured and simulated pulses, the shapes of the temporal profiles of a pulse can be estimated.

Through this research, it has been shown that one can predict the dynamics of the pulse knowing only the initial spectral and temporal profile of the input pulse and the refractive index of water. This technique can be applied to any pulse propagation through any linear dielectric medium.

REFERENCES

[1] U. Keller, "Recent developments in compact ultrafast lasers," Nature, **424**, 831-838, (2003)

[2] U. J. Gibson and U. Osterberg, "Optical precursors and Beer's law violations; non-exponential propagation losses in water," OPTICS EXPRESS, **13**, 2105-2110, (2005)

[3] S. H. Choi, U. Osterberg, "Obervation of optical precursors in water," PRL, **92**, 193903-1~193903-3, (2004) (1997)

[4] R. R. Alfano, J. L. Birman, X. Ni, M. Alrubaiee, and B. B. Das, "Comment on "Observation of optical precursors in water"," PRL, **94**, 239401-1, (2005)

[5] J. Li, D. R. Alexander, H. Zhang, U. Parali, D. W. Doerr, J. C. Bruce III, H. Wang, "Propagation of ultrashort laser pulses through water," OPTICS EXPRESS, **15**, 1939-1945, (2007)

[6] R. Buchner, J. Barthel and J. Stanber, "The dielectric relaxation of water between 0^{O}C and 35 ^{O}C," Chem. Phys. Letters., **306**, 57-63, (1999)

[7] D. Hovhannisyan, K. Stepanyan and R. Avayan, "Computational modeling of second-harmonic generation by a femtosecond laser pulse of a few optical cycles," J of Mod Optics, **52**, 97-107, (2005)

[8] K. S. Yee, "Numerical solution of initial boundary value problems involving Maxwell's equations in isotropic media," IEEE Trans. Antenna and Propagat., **17**, 585-589, (1966)

[9] A. Taflove and M. Brodwin, "Numerical solution of steady state electromagnetic scattering problems using the time-dependent Maxwell's equation," IEEE Trans. Microwave Theory Tech., **23**, 623-730, (1975)

[10] A. Taflove and S. Hagness, *Computational Electrodynamics*: The Finite Difference Time-Domain Method (Artech, Boston, MA, 2000)

[11] D. M. Sullivan, *Electromagnetic Simulation Using the FDTD Method* (Wiley-IEEE press, 2006)

[12] S. D. Gedney, "An anisotropic perfectly matched layer-absorbing medium for the truncation of FDTD lattice," IEEE Trans. Antennas Propag., **14**, 302-307, (1996)

[13] Y. Huang, and S. T. Ho, "Computational model of solid-state, molecular, or atomic media for FDTD simulation based on a multi-level multi-electron system governed by Pauli exclusion and Fermi-Dirac thermalization with application to semiconductor photonics," Optics Express, **15**, 3569-3587, (2006)

[14] P. Yang and K. N. Liou, "Finite-difference time domain method for light scattering by non spherical and inhomogeneous particles," in *Light Scattering by Nonspherical Particles: Theory, Measurements, and Applications*, M. I. Mishchenko, S. W. Hovenier, and L. D. Travis, eds., (Academic Press, San Diego, CA, 2000) pp. 173-221

[15] Y. Okawachi, A. D. Slepkov, I. H. Agha, D. F. Geraghty, and A. L. Gaeta, "Absorption of ultrashort optical pulses in water," J. Opt. Soc. Am. A, **24**, 3343-3347, (2007)

[16] R. M. Pope, and E. S. Fry, "Absorption spectrum (380-770 nm) of pure water. Ii. Integrating cavity measurements," Appl. Opt., **36**, 8710-8723, (1997)

[17] L. Kou, D. Labrie, and P. Chylek, "Refractive indices of water and ice in the 0.65-2.5 μm spectral range," Appl. Opt., **32**, 3531-3540, (1997)

[18] A. H. Harvey, J. S. Gallagher, and J. M. H. Levelt Sengers, "Revised formulation for the refractive index water and stream as a function of wavelength, temperature and density," J. Phys. Chem Ref. Data, **27**, 761-774, (1998)

[19] The International Association for the Properties of Water and Steam (IAPWS). Retrieved from http://www.iapws.org/

[20] J. D. Jackson, *Classical Electrodynamics*, 2nd ed., (Wiley, New York, 1975) (1997)

VITA

Name: Joong-Hyeok Byeon

Address: 423-063
KyungGiDo KwongMyungSi Haan 3 Dong
Haan apt 602-1508

Email Address: Joong_Hyeok@hotmail.com

Education: B.S., Physics, Ajou University, Rep of Korea, 1994
M.S., Physics, Seoul National University, 1996
M.S., Physics, Texas A&M University, 2008